ATOMIC AND MOLECULAR QUANTUM MECHANICS BY THE PATH INTEGRAL MOLECULAR DYNAMICS METHOD

Dafna SCHARF, Joshua JORTNER
School of Chemistry, Tel-Aviv University, 69978 Tel Aviv, Israel

and

Uzi LANDMAN
School of Physics, Georgia Institute of Technology, Atlanta, GA 30332, USA

Received 16 August 1986

The quantum path integral molecular dynamics method was applied to studies of excess electron localization by a Na^+ ion and by a NaCl molecule. Spatial and energetic characterization of the ground state of the excess electron compare favorably with results of model potential calculations for Na and with SCF CI calculations for $NaCl^-$.

1. Introduction

The properties of an excess electron in condensed matter systems [1–3] and in finite clusters [4] are of fundamental importance. Excess electron states in dense fluids [5–7] and in clusters [8] have recently been explored using the quantum path integral formulation of statistical mechanics [9,10] utilizing the quantum path integral molecular dynamics method (QUPID) [5–10], as well as the Monte Carlo technique [11]. While extensive data are available concerning excess electron states in fluids [1–3], experimental information concerning excess electron in clusters [4] is meagre. Recent computer simulations, which demonstrated the energetic stability of a localized electron state and the possibility of isomerization induced by electron localization in alkali halide ionic clusters [8], are not yet amenable to confrontation with experiment. In this note we apply the QUPID method to electron binding to two simple systems, which involve the elementary ingredients of the alkali halide (AH) system used in previous studies [8], i.e. a Na^+ ion and a NaCl molecule. These calculations were undertaken to demonstrate that one can obtain quantitative information for the energetics and for the charge distribution of an excess electron attached to small ionic systems, establishing confidence in the QUPID method in conjunction with the pseudopotential formalism [12–14] for electron–ion interactions, and thus providing reliable results for electron localization in ionic clusters [8].

2. Methodology

The QUPID method was used to simulate an electron interacting with a Na^+ ion or with a NaCl (AH) molecule. While the heavy atoms, whose thermal wavelength is very small, are reasonably treated by classical mechanics, a quantum treatment is essential for the electron. The partition function Z for a single electron in the external potential of the ions V_e is

$$Z = \mathrm{Tr}[\exp(-\beta H_e)] , \quad (1)$$

where $H_e = K_e + V_e$, K_e is the electron kinetic energy and $\beta = 1/kT$. An approximate expression for the partition function, which is amenable to numerical computations, can be obtained [10] through the use of Trotter's formula and the free-particle propagator

0 009-2614/86 $ 03.50

in coordinate representation, yielding

$$Z \approx \mathrm{Tr}[\exp(-\beta K_e/P)\exp(-\beta V_e/P)]^P = \left(\frac{Pm}{2\hbar^2\beta\pi}\right)^{3P/2} \times \int \ldots \int \mathrm{d}\boldsymbol{r}_1 \ldots \mathrm{d}\boldsymbol{r}_P \exp[-\beta V_{\mathrm{eff}}(\boldsymbol{r}_1 \ldots \boldsymbol{r}_P)] , \quad (2)$$

where m is the mass of the electron and the effective potential is

$$V_{\mathrm{eff}} = \sum_{i=1}^{P}\left(\frac{Pm}{2\hbar^2\beta^2}(\boldsymbol{r}_i - \boldsymbol{r}_{i+1})^2 + \frac{1}{P}V_e(\boldsymbol{r}_1 \ldots \boldsymbol{r}_P)\right). \quad (3)$$

The external potential V_e incorporates the electron–ion interactions corresponding to the e–Na^+ interaction for Na and the sum of e–Na^+ and e–Cl^- interactions for the $NaCl^-$ system. Core exclusion effects are very important for the e–Na^+ interaction and are dealt with through a local pseudopotential, which can be replaced by a two-parameter simple model potential [13,14]. The e–Na^+ model potential, V_{eA}, for the electron chain is [14]

$$V_{eA} = -\frac{1}{P}\sum_{i=1}^{P}\frac{e^2}{r_{iA}}, \qquad r_{iA} \geq R_c ,$$

$$= -\frac{1}{P}\sum_{i=1}^{P}\frac{e^2}{R_c}\theta(R_c - r_{iA}) , \quad r_{iA} \leq R_c , \quad (4)$$

where R_c is a cutoff radius and θ is the Heaviside step function. For Na^+ we take $R_c = 3.22$ au [14].

The e–Cl^- interaction, V_{eH}, is modelled by a Coulomb repulsion from the closed-shell anion and thus the core exclusion contribution is expected to be very small. The Coulomb interaction is complemented by the electron-induced polarization interactions, which is operative at distances larger than the ionic radius, R_I, of the Cl^- ion, and is corrected for the "self-energy" of the induced dipole. This core polarizability contribution accounts for electron correlation effects.

$$V_{eH} = \frac{1}{P}\sum_{i=1}^{P}\left(\frac{e^2}{r_{iH}} - \frac{e^2\alpha_H}{2r_{iH}^4}\right), \quad r_{iH} \geq R_I ,$$

$$= \frac{1}{P}\sum_{i=1}^{P}\frac{e^2}{r_{iH}}, \qquad r_{iH} < R_I , \quad (5)$$

where α_H is the anion polarizability. We note in passing that the polarizability contribution was not incorporated in the e–Na^+ potential, eq. (4), as the model potential parameters were chosen to fit the spectroscopic data.

For the interaction between the ions, V_{AH}, two model potentials were used. In the simplest form the interaction is a sum of the Coulomb attraction and the Born–Mayer repulsion with the parameters $\tilde{A}$ and ρ given by Fumi and Tosi (FT) [15],

$$V_{AH} = -e^2/R_{AH} + \tilde{A}_{AH}\exp(-R_{AH}/\rho) . \quad (6)$$

The second form for the interionic potential is based on a truncated Rittner model, which was developed by Brumer and Karplus (BK) [16]. It accounts for the charge-induced-dipole interaction via effective ionic polarizability α_H and α_A of the anion and the cation, respectively, and for the van der Waals attraction at short distances. The potential parameters $\tilde{A}'$, ρ' and c were given by BK [16]

$$V_{AH} = -e^2/R_{AH} + \tilde{A}'_{AH}\exp(-R_{AH}/\rho') - e^2(\alpha_A + \alpha_H)/2R_{AH} - c/R_{AH}^6 . \quad (7)$$

The average energy of the electron is evaluated at thermal equilibrium from the exact relation

$$E_e = -\partial \ln Z/\partial\beta , \quad (8)$$

resulting in

$$E_e = \mathrm{KE}_e + \mathrm{PE}_e , \quad (9)$$

where

$$\mathrm{KE}_e = \frac{3P}{2\beta} - \frac{Pm}{2\hbar^2\beta^2}\left\langle \sum_{i=1}^{P}(\boldsymbol{r}_i - \boldsymbol{r}_{i+1})^2 \right\rangle \quad (10a)$$

and

$$\mathrm{PE}_e = \frac{1}{P}\sum_{i=1}^{P}V_e(\boldsymbol{r}_1 \ldots \boldsymbol{r}_P) . \quad (10b)$$

KE_e is the kinetic energy and PE_e represents the potential energy of the electron. An estimator for the kinetic energy, which avoids the errors incurred by the subtraction of large quantities was advanced by Herman et al. [17],

$$\mathrm{KE}_e = \frac{3}{2\beta} + \frac{1}{2P}\sum_{i=1}^{P}\left\langle\left(\frac{\partial V_{eA}}{\partial \boldsymbol{r}_i} + \frac{\partial V_{eH}}{\partial \boldsymbol{r}_i}\right)\cdot(\boldsymbol{r}_i - \boldsymbol{r}_P)\right\rangle . \quad (11)$$

The kinetic energy of the electron consists of the free particle term and the kinetic energy of interaction with the ions. Together with the energies of the classical particles, the energy of the system is

$$E = 3N/2\beta + \langle V_{AH} \rangle + \mathrm{KE_e} + \langle V_{eA} \rangle + \langle V_{eH} \rangle \,. \quad (12)$$

The averages, which are denoted by the angular brackets, are taken over the Boltzmann distribution as defined by eqs. (2) and (3). In the classical isomorphism the statistical ensemble averages can be replaced by averaging over trajectories generated via classical molecular dynamics by the Hamiltonian

$$H = \sum_{i=1}^{P} m^* \dot{\boldsymbol{r}}_i^2 + M_A \dot{\boldsymbol{R}}_A^2 + M_H \dot{\boldsymbol{R}}_H^2 + V_{eA} + V_{eH} + V_{AH} + \sum_{i=1}^{P} \frac{Pm}{2\hbar^2\beta^2} (\boldsymbol{r}_i - \boldsymbol{r}_{i+1})^2 \,. \quad (13)$$

Since the equilibrium thermodynamic averages do not depend on the masses which appear in the kinetic energy term for the pseudo-particles, an arbitrary mass can be assigned to m^*. We note that the trajectories in the QUPID method do not correspond to the real-time dynamical evolution of the system and the method is limited to the calculation of equilibrium properties.

3. Numerical procedure

The preparation of the systems in thermal equilibrium (50 K) consisted of several stages. Initially, the electron bead particles ($P=998$) which were distributed over a sphere around the Na^+ (or the NaCl), were allowed to approach the ion(s), while the kinetic energy was controlled. Then, constant energy trajectories for the MD Hamiltonian (eq. (13)) were generated for a large number of integration steps (5×10^4 in Na and 7.5×10^4 in $NaCl^-$) before averaging was performed over the subsequent integration steps (2×10^4 in Na and 5×10^4 in $NaCl^-$). Energy was conserved in all runs, to better than 0.05% over 10^5 integration steps.

Table 1
QUPID calculations for $Na^+ + e$. Potential energy (PE), kinetic energy (KE) and total binding energy (BE) of an electron to a Na^+ ion compared with the experimental ionization potential (IP) of a sodium atom. The energy variance is given in parentheses. All energies are given in hartree units

	PE	KE	BE	IP experiment [a]
eq. (10)	−0.2504 (0.0003)	0.0657 (0.008)	0.1847 (0.008)	0.1889
eq. (11)	−0.2504 (0.0003)	0.0654 (0.0001)	0.1850 (0.0004)	

[a] See ref. [18].

4. Results and discussion

4.1. $e + Na^+$

The calculated energies for the binding of the electron at 50 K are given in table 1. The kinetic energy value using the estimator given in eq. (11), is more accurate than that obtained from eq. (10a), in accord with previous results [8,11]. The binding energy compares well with the experimental results and with conventional quantum-mechanical calculations [19] and pseudopotential calculations [13], inspiring confidence in the QUPID method and the model potential which was employed for the alkali-ion–electron interaction. In fig. 1a we show a snapshot of the electron bead particles projected on a 2D plane, exhibiting a uniform spherical distribution around the sodium ion. The normalized radial distribution for the positions of the pseudo-particles (beads) around the Na^+ is given by the probability distribution function

$$g(r) = \frac{1}{P} \sum_r n(r, \Delta r) \,, \quad (14)$$

where $n(r, \Delta r)$ is the number of pseudo-particles in a shell of radius r and thickness Δr, centered around the ion. $g(r)$ is compared with numerical information for the Hartree–Fock–Slater radial 3s wavefunction for the valence electron in sodium [19]. In fig. 2 we show the histogram of the averaged radial distribution of the bead particles along with the 3s probability distribution for the Na atom.

The extent of localization of the electron is closely related to the distribution of distances between the pseudo-particles, which represent points on the elec-

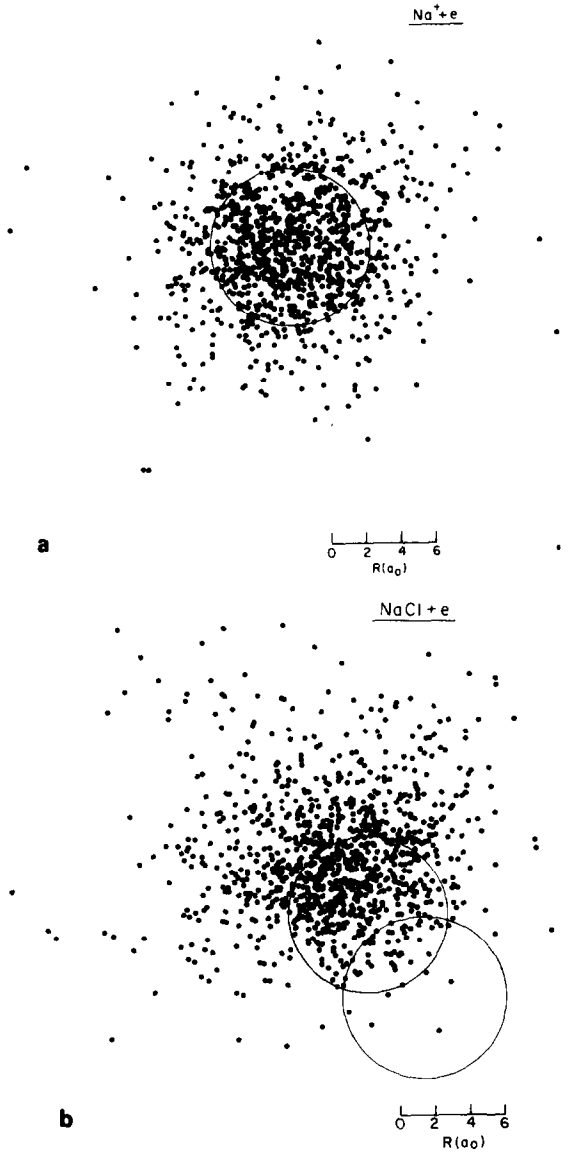

Fig. 1. Snapshots of the electron bead particles projected on a 2D plane. (a) $e+Na^+$, (b) e+NaCl. The large open circles correspond to the cutoff radius in the local model potential for the Na^+ core and for the ionic radius in Cl^-. The lower circle corresponds to the Cl^- anion.

tron path. We can estimate the "breadth" of the quantum particle by examining moments of the pseudo-particle distribution. We define

$$R_T^f=\left(\frac{P}{P-1}\sum_{i=1}^{P}\langle(r_i-r_{i+1})^2\rangle\right)^{1/2},$$

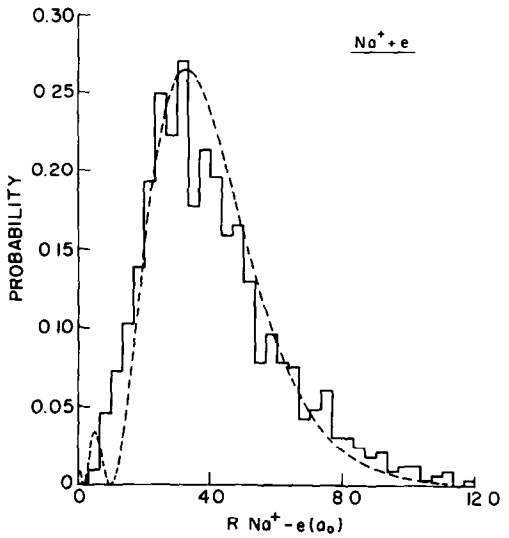

Fig. 2. Histogram of the calculated radial distribution for the electron bead particles for $e+Na^+$. The probability distribution for the 3s orbital in Na from a Hartree–Fock calculation [19] is given by the dashed line.

which for a free electron with the distances between pseudo-particles obeying Gaussian statistics yields $R_T^f=3^{1/2}\lambda_T$, where $\lambda_T=\beta\hbar^2/m$ is the thermal wavelength of the electron. At 50 K, $\lambda_T\approx 80\ a_0$ and $R_T^f=120\ a_0$, being close to the value of $R_T=136\ a_0$, which we find for the $e-Na^+$ system. The interactions of the quantum particle with the ions tend to confine the pseudo-particle chain to a "localized form". The second moment of the bead distribution is proportional to the gyration radius of the chain:

$$R_g^2=\frac{1}{2P^2}\left\langle\sum(r_i-r_j)^2\right\rangle. \tag{15}$$

We have found $R_g=4.53\pm0.04\ a_0$ with the three components, $R_{gx}=2.64\pm0.05\ a_0$, $R_{gy}=2.66\pm0.4\ a_0$ and $R_{gz}=2.55\pm0.12\ a_0$, exhibiting an isotropic electron distribution centered around the ion. The value for R_g is considerably lower than λ_T.

The compression of the pseudo-particle chain (degree of localization) can be analyzed in terms of the self-pair time-correlation function [20]:

$$R^2(t-t')=\langle|r(t)-r(t')|^2\rangle. \tag{16}$$

$R(t-t')$ is the rms value of the displacement between

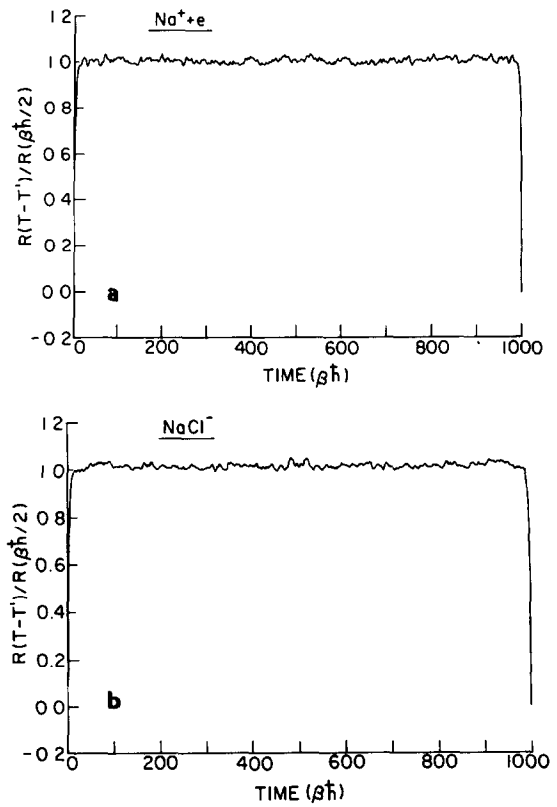

Fig. 3. The self-pair time-correlation function. The values of $R(t-t')$ are normalized to the corresponding characteristic length $R(\beta\hbar/2)$. (a) e+Na^+, (b) e+NaCl.

two points on the electron path separated by an imaginary time increment $0 \leqslant t-t' \leqslant \beta\hbar$. The characteristic size of such a chain is given by $R(\beta\hbar/2)$ [20]. A localized configuration of the quantum particle chain corresponds to a pronounced deviation of R from the free-particle value. We have found that $R(\beta\hbar/2) = 2.53\ a_0$, whereas $R_{\text{free}} = (\frac{3}{4})^{1/2}(\beta\hbar^2/m)^{1/2} \approx 69\ a_0$. Accordingly, the localization condition is well met, as is expected. In fig. 3a we plot $R(t-t')$ versus time. For a localized state, fluctuations in $R(t-t')$ are inhibited due to the dominance of the ground-state contribution, yielding independence of $R(t-t')$ on t, except for small intervals of magnitude τ near 0 and $\beta\hbar$. The range of variation of $R(t-t')$ at the edges of the interval (in $\beta\hbar$ units) is equal to the reciprocal of the mean excitation energy to the manifold of the excited states, i.e. mainly to the first excited state. We have found this mean excitation energy to be 2.1 ± 0.2 eV, which agrees favorably with the experimental values 2.102 and 2.104 eV for the lowest electronic excitations of Na.

4.2. e+NaCl

The binding energy of the electron to the NaCl diatomic molecule was calculated by taking the difference between the total energy of $NaCl^-$ and of NaCl. The calculated energies and equilibrium distances are given in table 2 for $NaCl^-$ and in table 3 for NaCl. The calculations for the NaCl molecule were performed by classical MD. We have found the calculated excess electron binding energy, i.e. the electron affinity of NaCl to be in the range EA = 0.9–1.0 eV with an uncertainty of ± 0.1 eV. The equilibrium distance of $NaCl^-$ is calculated to be $R_e = 4.66$–$4.84\ a_0$. The electron affinity calculation of Jordan et al. for $NaCl^-$ in an unrestricted Hartree–Fock method [22] resulted in EA = 0.65 eV for the equilibrium ion separation $R_e = 4.74\ a_0$. The agreement between the Hartree–Fock result [22] and ours for EA and for R_e is as good as can be expected in view of the uncertainties inherent in both the self-consistent field method and in our use of simple model potentials.

Table 2
QUPID calculations for NaCl–e. Kinetic energy (KE), potential energy (PE), total energy (E_{tot}) for the classical ions and for the electron. Under electron K_{est} and KE are the kinetic energies according to eqs. (11), (10), respectively. Total energy of NaCl+e (E_{tot}) and the binding energy for the electron (BE). Equilibrium distance (R_e). Numbers in parentheses represent the standard deviation. Energies in hartrees and distance in a_0. $T = 50$ K

	BK (eq. (7))		FT (eq. (6))	
ions				
KE	3.3×10^{-4}	(2×10^{-4})	5×10^{-4}	(2×10^{-4})
PE	0.1953	(6×10^{-4})	0.137	(1×10^{-3})
E_{tot}	0.1950	(8×10^{-4})	0.136	(1×10^{-3})
electron				
KE_{est}	0.048	(3×10^{-3})	0.0497	(3×10^{-3})
KE	0.048	(9×10^{-3})	0.0496	(8×10^{-3})
PE	0.085	(2×10^{-3})	0.0900	(2×10^{-3})
E_{tot}	0.037	(5×10^{-3})	0.0410	(5×10^{-3})
NaCl+e				
E_{tot}	0.232	(5×10^{-3})	0.2374	(6×10^{-3})
BE	0.034	(5×10^{-3})	0.0382	(6×10^{-3})
R_e	4.66	(4×10^{-2})	4.84	(7×10^{-2})

Table 3
Molecular dynamics calculations for NaCl. Potential energy (PE), kinetic energy (KE), total energy (E_{tot}) and equilibrium distance R_e. Numbers in parentheses represent the standard deviation. Energies in hartrees, R_e in a_0. The experimental data [21] are given for a monomer in low-pressure gas phase ($T \approx 950$ K)

	PE	KE	E_{tot}	R_e
FT (eq. (7))				
$T=50$ K	-0.1975098 (5×10^{-7})	7.94×10^{-5} (4×10^{-7})	-0.1974304 (9×10^{-7})	4.370 (5×10^{-3})
$T=950$ K	-0.19750 (1×10^{-5})	0.001500 (6×10^{-6})	-0.19600 (2×10^{-5})	4.38 (2×10^{-2})
BK (eq. (8))				
$T=50$ K	-0.1992323 (5×10^{-7})	7.99×10^{-5} (4×10^{-7})	-0.1991524 (9×10^{-7})	4.550 (5×10^{-3})
$T=950$ K	-0.19922 (1×10^{-5})	0.00150 (1×10^{-5})	-0.19772 (2×10^{-5})	4.56 (1.6×10^{-2})
experimental	-	-	-0.2047	4.4598

Using the BK potential we estimate the relative contributions of the various components to the energy of NaCl, with the Born–Mayer interactions accounting for $\approx 90\%$, the charge-polarizability interactions being $\approx 9.5\%$, while the van der Waals interaction contributions contributing $\approx 0.5\%$ to the PE of the ions. For the electron–NaCl interactions, the Coulomb interaction accounts for $\approx 98\%$, and the induced polarization interaction yields $\approx 2\%$ of the potential energy of the electron. The electron kinetic energy consists of a $\approx 95\%$ contribution from the Coulomb terms, 4.5% from the induced dipole interaction and $\approx 0.5\%$ from the free-particle kinetic energy.

In fig. 1b we show a snapshot of the electron chain of pseudo-particles projected on a 2D plane. In fig. 4 we show the radial distribution of the electron bead around the Na^+ ion and around the Cl^- ion. It is evident that the electron is mainly localized around the Na^+ ion, being strongly repelled from the Cl^- core, as expected. The gyration radius $R_g = 5.23\text{–}5.03 \pm 0.05\ a_0$ is larger than the gyration radius for the 3s electron in Na. The radial distribution exhibits a peak at a larger distance from the core of the Na^+ ion relative to the 3s electron in Na. $R(\beta\hbar/2) \approx 2.75\ a_0$ is much smaller than λ_T. Thus the localization condition is well met, as is evident from fig. 3b, where we show $R(t-t')$ versus time.

We conclude that $NaCl^-$ constitutes a relatively stable molecule, which is in accord with the SCF calculations [22]. The electron distribution possesses cylindrical symmetry with the intermolecular bond direction a the axial symmetry direction. The electron distribution is peaked behind the Na^+ and away from the Cl^- ion, with the distance between the maximum of the electron distribution and the Cl^- being about twice its distance to the Na^+ ion. We find that the degree of localization of the electron in the $NaCl^-$ molecule is diminished in comparison with that found in the e–Na^+ system. Finally, the bond length in the $NaCl^-$ molecule is large in comparison with that of the neutral NaCl molecule.

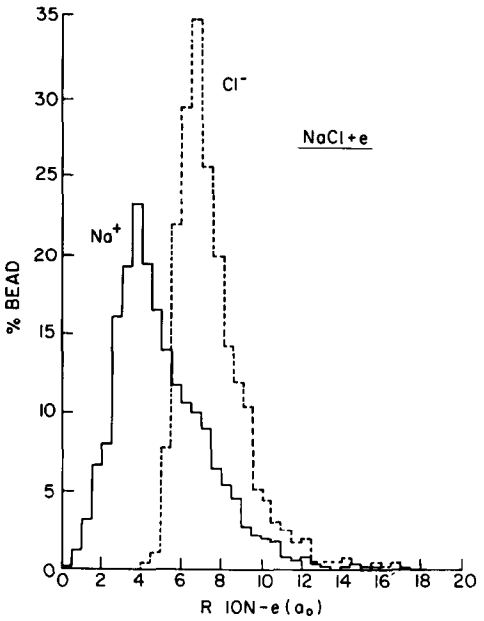

Fig. 4. Histograms of the radial distribution in the e+NaCl system for the electron bead particles around the Na^+ core (solid line) and the Cl^- core (dashed line).

We have demonstrated that the QUPID method in

conjunction with model potentials constitutes a reliable scheme for the exploration of electron binding to NaCl, and most likely to other alkali halide molecules. This conclusion inspires confidence in the application of this approach to the interesting problem of electron localization in alkali halide clusters which, as we have shown recently, can result in bulk states, surface states, reactive dissociation and cluster isomerization induced by electron attachment [8].

Acknowledgement

This work was supported in part by the US DOE, Grant No. DE-FG05-86ER45234 (UL) and by the United States Army through its European Research Office (JJ).

References

[1] N.F. Mott and E.A. Davis, in: Electronic processes in non-crystalline materials (Clarendon Press, Oxford, 1971).
[2] E.J. Hart and M. Anbar, eds., The hydrated electron (Wiley, New York, 1970).
[3] J. Jortner and N.R. Kestner, eds., Electron in fluids (Springer, Berlin, 1973).
[4] J. Jortner, Ber. Bunsenges. Physik. Chem. 88 (1984) 188.
[5] M. Parrinello and A. Rahman, J. Chem. Phys. 80 (1984) 86.
[6] J. Bartholomew, R.W. Hall and B.J. Berne, Phys. Rev. B32 (1985) 548.
[7] C.D. Jonah, C. Romero and A. Rahman, Chem. Phys. Letters 123 (1986) 209.
[8] U. Landman, D. Scharf and J. Jortner, Phys. Rev. Letters 54 (1985) 1860.
[9] R.P. Feynman and A.R. Hibbs, Quantum mechanics and path integrals (McGraw-Hill, New York, 1965).
[10] L.S. Schulman, Techniques and applications of path integrals (Wiley, New York, 1981).
[11] D.L. Freeman and J.D. Doll, J. Chem. Phys. 82 (1985) 462.
[12] V. Heine, Solid State Phys. 24 (1970) 1.
[13] J.V. Abarenkov and V. Heine, Phil. Mag. 12 (1965) 529.
[14] R.W. Shaw, Phys. Rev. 174 (1968) 769.
[15] F.G. Fumi and M.P. Tosi, J. Phys. Chem. Solids 25 (1964) 31, 45.
[16] P. Brumer and M. Karplus, J. Chem. Phys. 58 (1973) 3903.
[17] M.F. Herman, E.J. Bruskin and B.J. Berne, J. Chem. Phys. 76 (1982) 5150.
[18] R.C. Weast, ed., Handbook of chemistry and physics, 62nd Ed. (CRC Press, Boca Raton, 1982).
[19] F. Herman and S. Skillman, Atomic structure calculations (Prentice-Hall, Englewood Cliffs, 1963).
[20] A.L. Nichols III, D. Chandler, Y. Singh and D.M. Richardson, J. Chem. Phys. 81 (1984) 5109.
[21] E.J. Mawhorte, M. Fink and J.G. Hartley, J. Chem. Phys. 83 (1985) 4418.
[22] K.D. Jordan and J.J. Wendoloski, Mol. Phys. 35 (1978) 223.